

---

# UUKG: Unified Urban Knowledge Graph Dataset for Urban Spatiotemporal Prediction

---

Yansong Ning<sup>1</sup>, Hao Liu<sup>1,2\*</sup>, Hao Wang<sup>3</sup>, Zhenyu Zeng<sup>3</sup>, Hui Xiong<sup>1,2</sup>

<sup>1</sup> AI Thrust, The Hong Kong University of Science and Technology (Guangzhou)

<sup>2</sup> CSE, The Hong Kong University of Science and Technology

<sup>3</sup> Alibaba Cloud Intelligence Group

yning092@connect.hkust-gz.edu.cn liuh@ust.hk

cashenry@126.com zhenyu.zzy@alibaba-inc.com xionghui@ust.hk

## Abstract

Accurate Urban SpatioTemporal Prediction (USTP) is of great importance to the development and operation of the smart city. As an emerging building block, multi-sourced urban data are usually integrated as urban knowledge graphs (UrbanKGs) to provide critical knowledge for urban spatiotemporal prediction models. However, existing UrbanKGs are often tailored for specific downstream prediction tasks and are not publicly available, which limits the potential advancement. This paper presents UUKG, the unified urban knowledge graph dataset for knowledge-enhanced urban spatiotemporal predictions. Specifically, we first construct UrbanKGs consisting of millions of triplets for two metropolises by connecting heterogeneous urban entities such as administrative boroughs, POIs, and road segments. Moreover, we conduct qualitative and quantitative analysis on constructed UrbanKGs and uncover diverse high-order structural patterns, such as hierarchies and cycles, that can be leveraged to benefit downstream USTP tasks. To validate and facilitate the use of UrbanKGs, we implement and evaluate 15 KG embedding methods on the KG completion task and integrate the learned KG embeddings into 9 spatiotemporal models for five different USTP tasks. The extensive experimental results not only provide benchmarks of knowledge-enhanced USTP models under different task settings but also highlight the potential of state-of-the-art high-order structure-aware UrbanKG embedding methods. We hope the proposed UUKG fosters research on urban knowledge graphs and broad smart city applications. The dataset and source code are available at <https://github.com/usail-hkust/UUKG/>.

## 1 Introduction

Urban SpatioTemporal Prediction (USTP) aims to forecast future urban dynamics by simultaneously capturing the spatial and temporal autocorrelations from past observations. Recently, with the development of machine learning technologies and the collection of large-scale urban data, USTP has achieved remarkable progress in various urban predictive tasks, such as traffic management, pollution monitoring, and emergency response [1, 2, 3]. USTP has become an essential service of the modern smart city.

In prior literature, many efforts have been devoted to improving the USTP performance by exploiting latent knowledge from diverse urban data sources [4]. In particular, one commonly used approach is manually extracting features from different datasets to integrate additional information.

---

\*Corresponding author.

For example, Tompson *et al.* [5] and Chen *et al.* [6] customize urban features from external dataset for crime prediction and bike trip prediction. However, these approaches heavily rely on a deep understanding of the application domain and are labor-intensive. Recently, inspired by the success of the Knowledge Graph (KG) in natural language processing tasks, the urban knowledge graph has been adopted to improve USTP. For instance, Wang *et al.* [7] construct a dedicated spatiotemporal knowledge graph by regarding trajectory and timestamp as entities to improve trajectory prediction. Liu *et al.* [8] construct user check-in relations to help mobility prediction. However, existing UrbanKGs are **task-specific and none of them is publicly available**, which discourages researchers from adopting it for their own work and thus limits the flourishing of knowledge-enhanced urban spatiotemporal prediction.

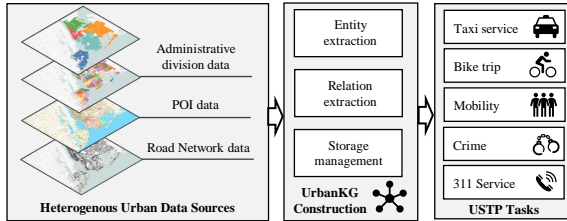


Figure 1: The generation process of UUKG.

Therefore, an open-sourced and multifaceted urban knowledge graph dataset compatible with various USTP tasks is necessary to be proposed. It is a non-trivial problem due to the following two challenges. (1) *How to construct unified urban knowledge graphs?* The urban data collected from different devices and providers describe the urban system from different aspects and granularities. They are usually disjoint datasets with different spatiotemporal ranges, which cannot be directly joint utilized for USTP. It is appealing to extract and align heterogeneous urban knowledge in a **unified graph organization** to satisfy diverse downstream USTP requirements. (2) *How to preserve complicated structural urban knowledge?* Existing UrbanKG-driven USTP approaches simply adopt general KG embedding methods or design complex task-specific module to project symbolic entities and relations into low-dimensional embeddings, which **fails to preserve unique structural patterns** in the urban knowledge graph. As illustrated in Figure 2, the urban knowledge graph includes diverse structures such as hierarchy and cycle. It is crucial to capture such high-order semantic knowledge to empower downstream spatiotemporal prediction tasks.

To address the aforementioned challenges, in this study, we present an Unified Urban Knowledge Graph (UUKG) dataset for knowledge-enhanced urban spatiotemporal predictions. Figure 1 illustrates the workflow of UUKG construction. For a given city, we first construct an Urban Knowledge Graph (UrbanKG) from multi-sourced urban data. By extracting and organizing entities (*e.g.*, POIs, road segments, *etc.*) into a multi-relational heterogeneous graph, UrbanKG encodes various high-order structural patterns in a unified configuration (*i.e.*, a multi-scale spatial hierarchy), which facilitates joint processing for various downstream USTP tasks. Moreover, we **qualitatively and quantitatively analyze these diverse high-order structures** (*i.e.*, hierarchies and cycles in Figure 2) to guide us in using tailored KG embedding methods to derive effective and generalizable knowledge representations. By learning **structure-aware embeddings** of entities and relations using state-of-art non-Euclidean space embedding models (*e.g.*, modeling hierarchies in hyperbolic space and capturing cycles in spherical space), the high-order structure information could be preserved in a proper way.

Finally, we conduct comprehensive experiments to benchmark diverse urban tasks, including the UrbanKG completion task, three urban flow prediction tasks, and two urban event prediction tasks. The empirical studies not only validate the effectiveness of the unified urban knowledge graph for improving various USTP tasks, but also uncover the high-order structures within UrbanKG, with proper modeling, can further strengthen the urban spatiotemporal prediction performance.

Our contributions are summarized as follows:

- We propose UUKG, **the first open-source UrbanKG dataset** for knowledge-enhanced urban spatiotemporal predictions. As a pilot study, we envision our experiences and results offering exciting opportunities to advance previous USTP methods.
- We demonstrate **the importance of urban high-order structure modeling** for urban knowledge representation and investigate to use structure-aware KG embedding methods to capture them effectively.
- Extensive experiments on KG completion and five USTP tasks demonstrate the effectiveness of the constructed UrbanKG and verify modeling high-order structures is beneficial to urban spatiotemporal prediction.

Table 1: The statistics of raw datasets.

Dataset	Description	Sample format	Records	
			New York	Chicago
Administrative division	Boundary	[ <i>"New York"</i> , <i>range(40.50, 40.91, -74.25, -73.70)</i> ]	1	1
	# of Borough	[ <i>"Queens"</i> , <i>polygon(40.54 -73.96, ...)</i> ]	5	6
	# of Area	[ <i>"Jamaica"</i> , <i>"Queens"</i> , <i>polygon(40.69 -73.82, ...)</i> ]	260	77
Road network	# of Segment	[ <i>road id, road name, start junction, end junction, type, line range</i> ]	110,919	71,578
	# of Category	[ <i>191751, "Queens Boulevard", 59378, 4798, tertiary, line(40.73 -73.82, ...)</i> ]	5	5
	# of Junction	[ <i>junction id, junction type, coordinate</i> ]	62,627	37,342
	# of Category	[ <i>59378, crossing, coordinate(40.78 -73.98)</i> ]	5	6
POI	# of POI	[ <i>poi id, poi name, poi type, coordinate</i> ]	62,450	31,573
	# of Category	[ <i>34633854, "Empire State Building", corporation, coordinate(40.75, -73.99)</i> ]	15	15

## 2 UrbanKG Construction

We first introduce the datasets that will be used for urban knowledge graph construction and data preprocessing details, then we present the construction of urban knowledge graphs.

### 2.1 Data Collection and Preprocessing

We acquire urban knowledge for two large cities, New York and Chicago, from three data sources. Table 1 summarizes the statistics of the datasets.

**Administrative Division data.** The administrative division describes multi-level spatial entities that the government uses to make administrative decisions, which contains rich geographical information for USTP task [9, 10]. In this work, we collect three administrative divisions, *i.e.*, city, borough, and area. We first manually define the rectangular latitude and longitude boundaries for each city (*e.g.*, New York and Chicago). Then we collect borough and area data from NYC Gov <sup>2</sup> and CHI Gov <sup>3</sup>, the official websites of New York and Chicago. Each borough record contains a borough name and polygon boundaries. Each area record contains an area name, corresponding borough name, and the polygon boundaries. Example in Table 1 is a record of *"Jamaica"* area in the *"Queens"* borough.)

**Road Network Data.** The road network provides rich topology knowledge of the transportation system, which plays a critical role in various USTP tasks (*e.g.*, traffic congestion prediction [11] and traffic incident detection [12]). We utilize the rectangular of each city to query the corresponding road network data (road segments and road junctions) from Open Street Map (OSM <sup>4</sup>). Each road segment record contains a unique id, a road name, a start road junction id, a end road junction id, and line geographical range. Each road junction record contains a unique id, junction type and coordinate (latitude and longitude). Example in Table 1 is a road record of *"Queens Boulevard"*, and it starts from junction 594778 and ends at junction 4798.

**POI Data.** POI data contains urban contextual semantics, which have been widely adopted as auxiliary features to enhance USTP tasks (*e.g.*, traffic prediction[13] and crime prediction [14]). We collect POI data from OSM. We utilize the boundary of each city from the administrative division data to query the corresponding POI records through the open API provided by OSM. Each POI record consists of a unique id, a POI name, POI category and the coordinate. Example in Table 1 is a POI record where (40.75, -73.99) is the location and the POI is a *corporation*.

Before constructing the UrbanKG, we first preprocess the raw datasets. We filter out POIs and road networks that don't belong to any administrative borough or area in each city. Besides, we merge minority POI categories (*e.g.*, grandstand and canopy) to avoid potential long-tail issues. As records from different data sources are disjoint, we align each record according to the administrative areas.

### 2.2 Knowledge Graph Construction

Then we introduce the process of constructing the urban knowledge graph (UrbanKG).

**Definition 1 UrbanKG.** The UrbanKG is defined as a multi-relational graph  $\mathcal{G} = (\mathcal{E}, \mathcal{R}, \mathcal{F})$ , where  $\mathcal{E}$ ,  $\mathcal{R}$  and  $\mathcal{F}$  is the set of urban entities, relations and facts, respectively. In particular, facts are

<sup>2</sup><https://www.nyc.gov/>

<sup>3</sup><https://www.chicago.gov/>

<sup>4</sup><https://www.openstreetmap.org/>

Table 2: Major relations in UrbanKG.

Relation	Symmetric	Head & Tail Entity	Abbrev.	Relation	Symmetric	Head & Tail Entity	Abbrev.
POI Locates at Area	×	(POI, Area)	PLA	Junction Belongs to Road	×	(Junction, Borough)	JBR
Road Locates at Area	×	(Road, Area)	RLA	Borough Nearby Borough	✓	(Borough, Borough)	BNB
Junction Locates at Area	×	(Junction, Area)	JLA	Area Nearby Area	✓	(Area, Area)	ANA
POI Belongs to Borough	×	(POI, Borough)	PBB	POI Has POI Category	×	(POI, PC)	PHPC
Road Belongs to Borough	×	(Road, Borough)	RBB	Road Has Road Category	×	(Road, RC)	RHRC
Junction Belongs to Borough	×	(Junction, Borough)	JBB	Junction Has Junction Category	×	(Junction, JC)	JHJC
Area Locates at Borough	×	(Area, Borough)	ALB	-	-	-	-

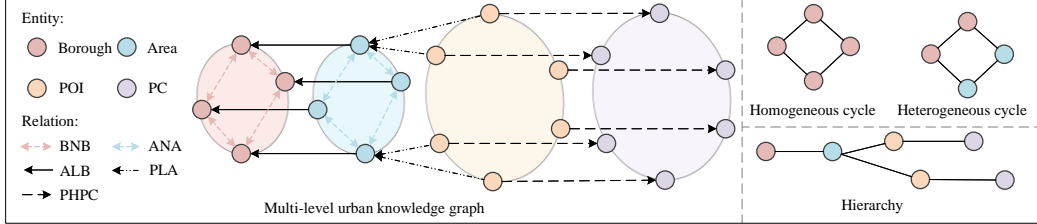


Figure 2: An illustrative example of the urban knowledge graph with diverse hierarchical and cyclic structure. There are four types of entities (Borough, Area, POI and POI Category (PC)) and five types of relations (BNB, ALB, ANA, PLA and PHPC).

defined as  $\mathcal{F} = \{\langle h, r, t \rangle \mid h, t \in \mathcal{E}, r \in \mathcal{R}\}$ , where each triplet  $\langle h, r, t \rangle$  describes that head entity  $h$  is connected with tail entity  $t$  via relation  $r$ . For example,  $\langle \text{Queen, Nearby, Brooklyn} \rangle$  represents the fact that Queen and Brooklyn are geographically adjacent.

The UrbanKG encodes diverse urban semantic knowledge such as the multi-level spatial adjacency (e.g., the Hammels area in Queens borough) and ontology (e.g., category of POIs and roads). We detail the entity and relation extraction below.

### 2.2.1 Entity Extraction

We extract 8 types of entities for UrbanKG: (1) **Administrative Borough (Borough)**. Borough describes high-level administrative boundaries of a city. For example, New York has five boroughs: Queen, Bronx, Brooklyn, Manhattan, and Staten Island. (2) **Functional Area (Area)**. Area refers to the subdivision of a city according to its function, such as residential, industrial, and commercial areas. (3) **Point-Of-Interest (POI)**. A POI is a basic functional unit and venue. For example, cinemas and hospitals are two common types of POIs and they are the places people often check in. (4) **Road Segment (Road)**. Road is the key element in the city and it forms the traffic network, which provides a reference and basis for human mobility. (5) **Road Junction (Junction)**. Junction is where two or more road segments intersect. It is important for the urban road network as they have a great impact on traffic capacity and safety. (6) **POI Category (PC)**. POI category describes the property and function of POI, such as finance, catering and so on. We define 15 categories of POI including finance, parking area, shopping, catering, and so on. (7) **Road Category (RC)**. Road category describes the features of the road segment, such as motorway, trunk and so on. We preserve the six-types of most frequent road segments including motorway (expressway or river-crossing tunnels), primary traffic road, secondary traffic road, tertiary traffic road, residential traffic road, and trunk (branch roads such as expressway outbound bypass roads). (8) **Junction Category (JC)**. Junction category helps distinguish several special types of road junctions, such as roundabout. We keep five types of road junction including motorway junction (road junction in expressway or river-crossing tunnel), traffic signal (road junction having traffic light), turning circle (road junction which is a roundabout), stop (road junction having stop signal) and crossing (road junction with no special type).

We report the detailed statistics of entities in Appendix A.1.

### 2.2.2 Relation Construction

As shown in Table 2, we define 13 relations for UrbanKG:

Table 3: Statistics of two UrbanKGs. We report graph hyperbolicity values  $\delta$  (always greater than or equal to zero while lower means more hierarchical) and the number of cycles.

Dataset	# Entity	# Relation	# Triplet	# Train	# Valid	# Test	# Cycle	# Hyperbolicity
NYC	236,287	13	930,240	837,216	46,512	46,512	1,090,884	$\delta = 0$
CHI	140,602	13	564,400	507,960	28,220	28,220	532,108	$\delta = 0$

**Geographic Inclusion.** This type of relation describes the geographical inclusion relations between entities. We extract 5 geographical inclusion relations for UrbanKG: (1) *POI/Road/Junction Locates at Area (PLA/RLA/JLA)*. Through these relations, we can obtain the fact between Area and POI/Road/Junction. For example, triplet  $\langle POI\ 32, PLA, Area\ 75 \rangle$  indicates that POI 32 is located in Area 75. (2) *POI/Road/Junction Belongs to Borough (PBB/RBB/JBB)*. Through these relations, we can obtain the fact between Borough and POI/Road/Junction. (3) *Area Locates at Borough (ALB)*. Through this relation, we can obtain the geographic inclusion relations between Area and Borough. For example, triplet  $\langle Area\ 75, ALB, Borough\ 1 \rangle$  explains that Area 75 belongs to Borough 1. (4) *Junction Belongs to Road (JBR)*. Through this relation, we can describe the Junction on which Road, thus could preserve the topology of the road network.

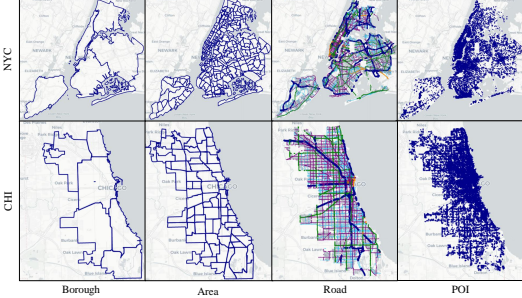


Figure 3: An illustrative visualization of the four UrbanKG entities in NYC and CHI.

**Geographic Adjacency.** This type of relation describes the geographical adjacency relations between entities. We extract 2 relations of this type for UrbanKG: (1) *Borough Nearby Borough (BNB)*. Through this relation, we can obtain the adjacency fact between Boroughs. (2) *Area Nearby Area (ANA)*. Through this relation, we describe the adjacency between Areas.

**Category.** This type of relation connects entities to the category they belong to. We extract three category relations for UrbanKG: (1) *POI Has POI Category (PHPC)*. (2) *Road Has Road Category (RHRC)*. (3) *Junction Has Junction Category (JHJC)*. For example, triplet  $\langle POI\ 32, PHPC, PC\ 4 \rangle$  indicates POI 32 belongs to the category PC 4.

### 2.2.3 UrbanKG Management

Following the above process, we obtain UrbanKGs for two large cities as shown in Table 3, *i.e.*, New York (NYC) and Chicago (CHI). To serve the large-scale knowledge graph with millions of triplets, we adopt Neo4j, a graph database system, to store, query, and update the UrbanKG. The data privacy issue is critical in smart city applications. In this study, the dataset we use doesn't include any user-level information. However, recent studies prove that sensitive individual information can be inferred from a few location check-ins [15]. Thus, we round the coordinate of each record to 100 meters to avoid potential information leakage when incorporating UrbanKG with other urban spatio-temporal data.

## 2.3 Visualization and Structural Analysis

As shown in Figure 3, the multi-level UrbanKG contains entities providing administrative division information (Borough & Area), traffic topology (Road network), and urban function distribution (POI), and they together form rich semantic information (*i.e.*, High-order hierarchy and high-order cycle) about the city.

**High-order Hierarchy.** Hierarchical information is ubiquitous in capturing knowledge from KG [16, 17, 18] since much knowledge is commonly organized hierarchically. For example, the hierarchy (*Borough*->*Area*->*POI*->*PC*) in Figure 2 organizes urban knowledge in a hierarchical way. Embracing and modeling such hierarchy empowers to uncover deeper semantics, *e.g.*, we can infer the main function of an area from the POI quantities and categories in this area. As shown in Table 3, we also quantitatively find the hyperbolicities [19] of two UrbanKGs are zero, which means that UrbanKGs

are not significantly different from a tree in terms of their geometric properties [20, 21]. Thus they are suitable to be represented in hyperbolic space [22, 19], where hierarchies can be losslessly embedded.

**High-order Cycle.** Cycle modeling is beneficial to improve knowledge representation [23, 24, 25] as it implies rich semantics of graphs. We find their existence in constructed UrbanKG by analyzing the topological structure. For example, the homogeneous cycle and heterogeneous cycle in Figure 2 uncover *Borough* geographic semantics and the geographic semantics of *Area* and *Borough*, respectively. Moreover, Table 3 counts the number of cycles in the two UrbanKG to further verify our analysis. Unlike hierarchy, these cycles are suitable to be modeled in spherical space [22, 26].

The qualitative and quantitative analysis reveal diverse high-order structural patterns in UrbanKG, and thus inspires us to leverage state-of-the-art high-order structure-aware knowledge graph embedding methods to extract tailored and comprehensive urban knowledge. For instance, UrbanKG can be embedded into hyperbolic space to capture hierarchies or into spherical space to model cycles.

### 3 Structure-aware UrbanKG Embedding

This section investigates the impact of different structure-aware embedding methods (*e.g.*, the hyperbolic space embedding module to capture hierarchy) on UrbanKG representation learning. We first give problem formulation of UrbanKG embedding and introduce how to utilize structure-aware embedding methods to represent those high-order structures within UrbanKG.

#### 3.1 Problem Formulation

Given the constructed UrbanKG  $\mathcal{G} = (\mathcal{E}, \mathcal{R}, \mathcal{F})$ , we aim to learn low-dimensional entity embeddings  $e_{\mathcal{E}}$  and relation embeddings  $e_{\mathcal{R}}$ , so that diverse high-order structure knowledge can be preserved to benefit various downstream USTP tasks.

#### 3.2 Experimental Setup

We compare the performance gap of different structure-aware knowledge graph embedding methods to investigate which approaches are suitable for modeling the unique structures in UrbanKG. The quality of UrbanKG embedding is evaluated using the link prediction task [27], which aims to predict the missing head or tail entity for a triplet  $\langle h, r, t \rangle$ . For each UrbanKG in Table 3, we follow standard data augmentation protocol [28] by adding inverse relations.

**Evaluation Metrics.** We report two popular metrics: (1) Mean reciprocal rank (MRR), the mean of inverse of correct entity ranking [29]. (2) Hits@K (K=1,3,10), the percentage of correct entities in top-K ranked entities [30, 31]. Note we filter out true triplets appearing in the training set during evaluation [30], because predicting a low rank for those triplets should not be penalized.

**Methods.** We utilize classical Euclidean methods as baselines and choose state-of-art structure-aware non-Euclidean approaches as backbones.

- **Euclidean Models:** (1) TransE [30] is a classical translational model; (2) DisMult [32] is a matrix factorization model; (3) ComplEx [33] is an extension of DisMult in complex space; (4) RotatE [34] is a rotation-based method in complex space; (5) MuRE [16] is a translational distance method with a diagonal relational matrix. (6) TuckER [35] is a tensor decomposition method. (7) QuatE [36] is a hypercomplex space embedding method.
- **Non-Euclidean Models:** (1) MuRP/MuRS [16] are hyperbolic or spherical model with diagonal relational matrix; (2) RotH/RefH [17] are hyperbolic embedding method with rotation or refelection. (3) AttH [17] is a hyperbolic embedding method combining rotation and reflection; (4) ConE [18] is a hyperbolic embedding method with transformation between hyperbolic cone; (5) M2GNN<sup>5</sup> [26] is a GNN-based product space embedding model which can model cycles and hierarchies at the same time. (6) GIE [37] is a product space model considering geometry interaction.

**Implement Details.** We implement all models using PyTorch. All experiments are conducted on eight NVIDIA RTX 3090 GPUs. The negative sampling size is fixed to 50. We conduct hyperparameters grid search by early stop on the validation sets and we report details in Appendix A.2.

<sup>5</sup>Due to the large scale of our UrbanKG, we didn't perform Graph Neural Updater when reproducing.

Table 4: Overall link prediction results on NYC and CHI dataset. We utilize E, C, S, H, P to denote the Euclidean, Complex, Spherical, Hyperbolic and Product space, respectively. Best results in each space are underlined.

Type	Space	Model	NYC				CHI			
			MRR	Hits@10	Hits@3	Hits@1	MRR	Hits@10	Hits@3	Hits@1
Euclidean models	E	TransE	.507	.563	.528	<u>.470</u>	.485	.556	.501	.436
	E	DisMult	.401	.478	.433	.355	.395	.479	.469	.394
	E	MuRE	<u>.516</u>	<u>.613</u>	<u>.545</u>	.468	<u>.493</u>	<u>.601</u>	<u>.536</u>	<u>.437</u>
	E	TuckER	.513	.609	.541	.466	.488	.584	.525	.423
	C	RotatE	.274	.363	.309	.220	.306	.385	.336	.258
	C	ComplEx	.259	.357	.305	.195	.304	.385	.337	.253
	C	QuatE	<u>.321</u>	<u>.388</u>	<u>.347</u>	<u>.282</u>	<u>.396</u>	<u>.490</u>	<u>.427</u>	<u>.345</u>
Non-Euclidean models	S	MuRS	<u>.528</u>	<u>.622</u>	<u>.552</u>	<u>.478</u>	<u>.501</u>	<u>.619</u>	<u>.536</u>	<u>.437</u>
	H	MuRP	<u>.545</u>	<u>.635</u>	<u>.570</u>	<u>.497</u>	<u>.519</u>	<u>.634</u>	<u>.555</u>	<u>.456</u>
	H	RotH	.526	.601	.550	.472	.511	.626	.548	.447
	H	RefH	.524	.610	.549	.473	.509	.629	.542	.451
	H	ATTH	.539	.603	.556	.503	.514	.610	.542	.463
	H	ConE	.542	.629	.563	.485	.513	.617	.535	<u>.465</u>
	P	M2GNN	.561	.638	.578	.521	.540	.651	.571	.481
	P	GIE	<u>.573</u>	<u>.665</u>	<u>.600</u>	<u>.523</u>	<u>.552</u>	<u>.660</u>	<u>.580</u>	<u>.498</u>

Table 5: Statistics of five USTP datasets in NYC and CHI.

Dataset	NYC					CHI				
	Taxi	Bike	Mobility	Crime	311 service	Taxi	Bike	Mobility	Crime	311 service
# of records	1,118,584	383,919	1,052,232	389,551	3,141,153	3,826,868	1,085,690	939,543	202,291	1,821,949
# of vertices	260	2,500	1,600	260	260	77	1,500	1,000	77	77
Time span	04/01/2020-06/31/2020		01/01/2021-31/12/2021			04/01/2019-06/31/2019			01/01/2021-31/12/2021	
Time interval	30 minutes		120 minutes			30 minutes			120 minutes	

### 3.3 Results

The embedding dimension is set to  $d = 32$  for all methods. The result in Table 4 indicates that almost all non-Euclidean (*i.e.*, hyperbolic and spherical space) embedding methods outperform Euclidean embedding methods, aligning with their capability to explicitly represent hierarchical and cyclic structures in urban knowledge graphs. Moreover, models that derive a product space (*i.e.*, combination of hyperbolic space and spherical space) to simultaneously capture hierarchies and cycles obtain the dominant performance. This can be attributed to the fact that UrbanKGs often exhibit both high-order hierarchies and cycles, making them suitable for simultaneous modeling in hyperbolic space and spherical space. We report detailed results, analysis and implement details in Appendix A.2.

## 4 Knowledge-enhanced Urban SpatioTemporal Prediction

In this section, we first give a formal problem statement of USTP, then introduce how to incorporate UrbanKG to enhance five USTP tasks. Finally, we extensively discuss the experimental results.

### 4.1 Problem Formulation

Let  $G = (V, E, A)$  denote a spatial network (*e.g.*, road network, sensor network, grid *etc.*), where  $V$  and  $E$  denote the set of vertices and edges. We use  $A$  to denote the adjacency matrix of the spatial network  $G$ . We further define the graph signal matrix  $X_G^{(t)} \in \mathbb{R}^{N \times C}$  for  $G$ , where  $C$  denotes the dimension of feature,  $N = |V|$  is the number of vertices, and  $X_G^{(t)}$  represents the observations of spatio network  $G$  at time step  $t$ . In general, the knowledge-enhanced urban spatiotemporal task aims to learn a multi-step prediction function  $f$  based on past observations and the UrbanKG  $\mathcal{G}$ ,

$$(X_G^{(t)}, X_G^{(t+1)}, \dots, X_G^{t+\tau}) = f((X_G^{(t-T)}, X_G^{(t-T+1)}, \dots, X_G^{t-1})), \mathcal{G}) \quad (1)$$

where  $\mathcal{G}$  is the UrbanKG we constructed,  $T$  is the input length of past observations,  $\tau$  is the future steps we aim to predict.

### 4.2 Incorporating UrbanKG Embedding

We demonstrate the effectiveness of UrbanKG by directly concatenating the learned UrbanKG embeddings with the graph signal matrix. In this work, we consider the following five USTP tasks.

**Taxi Service Prediction.** Taxi service prediction aims to predict future taxi inflow and outflow based on the historical taxi service. Following existing studies [38], we split the city into  $N$  disjoint areas, and connect the spatial network  $G$  based on area adjacency. Let  $C_{taxi}$  denote the two-dimensional feature vector (inflow and outflow). We incorporate the UrbanKG by concatenating the area embeddings with the taxi flow features,  $X_G^{(t)} \in \mathbb{R}^{N \times C_{taxi'}}$ , where  $C_{taxi'} = e_{Area} \parallel C_{taxi}$  and  $\parallel$  denotes the concatenation operation.

**Bike Trip Prediction.** Bike trip prediction aims to predict future inflow and outflow based on the historical bike trip. We sample  $N$  roads and connect the spatial network  $G$  based on road adjacency [13]. Let  $C_{bike}$  represent the two-dimensional feature vector (inflow and outflow). The road embedding  $e_{Road}$  is concatenated with it for UrbanKG fusion,  $X_G^{(t)} \in \mathbb{R}^{N \times C_{bike'}}$ , where  $C_{bike'} = e_{Road} \parallel C_{bike}$ .

**Human Mobility Prediction.** Human mobility prediction aims to predict future human inflow and outflow based on historical human mobility. Following existing studies [39], We choose  $N$  POIs and obtain the spatial network  $G$  based on their adjacency. Let  $C_{human}$  denote the two-dimensional feature vector (inflow and outflow). We integrate the UrbanKG by concatenating human mobility flow features with POI embedding,  $X_G^{(t)} \in \mathbb{R}^{N \times C_{human'}}$ , where  $C_{human'} = e_{POI} \parallel C_{human}$ .

**Crime Prediction.** Crime prediction is a binary prediction task based on the observation of historical crime events. Following existing studies [40], we split the city into  $N$  disjoint areas and connect the spatial network  $G$  according to area adjacency. Let  $C_{crime}$  denote the label of whether the crime occurs. We concatenate the Area embedding  $e_{Area}$  with crime feature,  $X_G^{(t)} \in \mathbb{R}^{N \times C_{crime'}}$ , where  $C_{crime'} = e_{Area} \parallel C_{crime}$ .

**311 Service Prediction.** 311 service prediction [41] is also a binary prediction task based on the observation of historical 311 complaint events. We obtain the spatial network  $G$  in the same way as crime prediction. Let  $C_{service}$  denote the label of the 311 complaint occurrence. We concatenate the Area embedding  $e_{Area}$  with its feature,  $X_G^{(t)} \in \mathbb{R}^{N \times C_{service'}}$ , where  $C_{service'} = e_{Area} \parallel C_{service}$ .

### 4.3 Experimental Setup

The result in Table 4 indicates that structure-aware non-Euclidean space embedding models can generate a better urban knowledge representation compared with Euclidean methods. To further verify modeling those high-order structures in Section 2.3 could enhance USTP tasks, we compare performance gaps for USTP tasks across different prediction time steps (3, 6, and 9) when using embeddings derived from different spaces. Next, we inject the embeddings from the space that yielded the greatest improvement into all downstream tasks and USTP models to confirm their benefits.

**Data Description.** The data statistics of five datasets are summarized in Table 5, and we provide the details of each dataset in Appendix A.3.

**Evaluation Metrics.** We utilize MAE and RMSE for regression tasks for evaluation [42] and use Micro-F1 and Macro-F1 [43] for classification tasks for evaluation.

**Methods.** We compare our approach with the following 9 methods: (1) Gate Recurrent Units (GRU) [44]; (2) Auto-Encoder (AE) [45]; (3) Long Short-Term Memory (LSTM) [46]; (4) SpatioTemporal Graph Convolution Network (STGCN) [47]; (5) Attention Based Spatial-Temporal Graph Convolutional Networks (ASTGCN) [48]; (6) Temporal Graph Convolutional Network (TGCN) [49]; (7) Multivariate Time Graph Neural Networks (MTGNN) [50]; (8) Adaptive Graph Convolutional Recurrent Network (AGCRN) [51]; (9) Hierarchical Graph Convolution Networks (HGNC) [52]. We incorporate UrbanKG embeddings from different spaces with USTP models as our approach, such as ASTGCN w/P and P denotes embedding from product space.

**Implement Details.** We split data with a ratio of 7:1:2 into training sets, validation sets and test sets. We use historical 12 time steps to predict the future 1 to 12 time steps. We provide implement details and more detailed results in Appendix A.4.

### 4.4 Results

**Comparison of UrbanKG Embedding Space Variants.** As depicted in Figure 4, we observe that the UrbanKG embeddings could enhance USTP tasks regardless of which spaces they come from.

Table 6: Performance gain of product space UrbanKG embedding on five spatiotemporal prediction tasks. All experimental results are the mean of 5 independent experiments repeated and the standard deviation (Std) are reported.

Model	NYC					CHI				
	Taxi MAE/RMSE	Bike MAE/RMSE	Mobility MAE/RMSE	Crime Micro/Macro-F1	311 service Micro/Macro-F1	Taxi MAE/RMSE	Bike MAE/RMSE	Mobility MAE/RMSE	Crime Micro/Macro-F1	311 service Micro/Macro-F1
GRU	1.802/3.587	0.920/1.115	1.003/1.318	-/-	-/-	3.372/8.895	1.431/2.619	1.157/1.800	-/-	-/-
LSTM	1.425/2.769	0.832/0.994	0.984/1.227	-/-	-/-	3.075/9.076	1.359/2.259	1.107/1.682	-/-	-/-
AE	1.399/2.484	0.701/0.898	0.956/1.233	56.42/52.12	65.68/59.64	3.313/11.64	1.416/2.706	1.148/1.721	57.49/57.27	54.67/55.34
STGCN	0.835/2.069	0.221/0.558	0.553/0.976	76.80/63.10	81.15/78.50	1.967/6.014	0.632/1.537	0.458/1.138	71.86/68.71	79.67/79.47
STGCN w/P	0.781/1.942	0.201/0.543	0.542/0.947	77.56/64.26	81.98/79.15	1.844/5.826	0.625/1.501	0.414/1.064	72.18/68.93	79.92/79.83
Std	0.001/0.000	0.006/0.002	0.000/0.001	0.001/0.000	0.001/0.001	0.003/0.002	0.006/0.012	0.004/0.001	0.008/0.003	0.002/0.003
Improv %	6.47%/6.14%	9.05%/2.69%	1.99%/2.97%	0.99%/1.84%	1.02%/0.83%	6.25%/3.13%	1.11%/2.34%	9.61%/6.50%	0.45%/0.32%	0.31%/0.45%
MTGNN	1.289/2.275	0.967/1.041	0.963/1.163	72.88/58.61	79.32/75.75	2.167/5.965	1.153/1.723	1.081/1.504	68.48/66.46	76.72/76.32
MTGNN w/P	1.183/2.118	0.920/1.021	0.891/1.083	73.47/60.02	80.28/77.85	1.975/5.882	1.083/1.641	0.983/1.399	71.73/68.65	78.29/77.99
Std	0.007/0.005	0.016/0.009	0.021/0.011	0.008/0.004	0.011/0.009	0.023/0.017	0.005/0.009	0.003/0.002	0.016/0.007	0.000/0.001
Improv %	8.22%/6.90%	4.86%/1.92%	7.48%/6.8%	0.81%/2.41%	1.21%/2.77%	8.86%/1.39%	6.07%/4.76%	9.07%/6.98%	4.75%/3.30%	2.05%/2.19%
AGCRN	1.315/2.391	0.958/1.038	0.945/1.148	65.98/60.62	75.68/69.64	2.403/7.277	1.187/1.768	0.213/1.281	64.14/63.35	71.18/67.07
AGCRN w/P	1.208/2.221	0.875/0.983	0.901/1.067	67.75/61.88	76.35/72.57	2.255/6.945	1.093/1.621	0.205/1.258	66.51/65.27	72.87/70.54
Std	0.016/0.021	0.035/0.011	0.006/0.005	0.000/0.000	0.001/0.003	0.019/0.026	0.007/0.011	0.004/0.015	0.001/0.000	0.000/0.000
Improv %	8.14%/7.11%	8.66%/5.30%	4.66%/7.06%	2.68%/2.08%	0.89%/4.21%	6.16%/4.56%	7.92%/8.31%	3.76%/1.80%	3.71%/3.03%	2.37%/5.17%
ASTGCN	0.832/2.141	0.231/0.579	0.566/0.973	76.69/61.62	80.82/77.45	1.849/5.323	0.745/1.822	0.505/1.259	71.77/68.45	79.18/78.93
ASTGCN w/P	0.805/2.012	0.220/0.564	0.558/0.944	76.94/62.34	81.28/78.85	1.822/5.198	0.690/1.754	0.463/1.191	72.22/68.90	78.29/77.98
Std	0.004/0.005	0.003/0.003	0.000/0.006	0.009/0.008	0.007/0.009	0.001/0.006	0.017/0.003	0.015/0.009	0.012/0.009	0.008/0.007
Improv %	3.25%/6.03%	4.76%/2.59%	1.41%/2.98%	0.33%/1.17%	0.57%/1.81%	1.46%/2.35%	7.38%/3.73%	8.32%/5.40%	0.63%/0.66%	1.15%/1.33%
TGCN	1.701/3.198	0.337/0.685	0.654/1.118	75.22/63.19	77.56/72.96	2.112/6.645	1.127/2.583	0.702/1.665	70.62/66.41	77.89/77.57
TGCN w/P	1.578/2.887	0.319/0.664	0.635/1.054	76.01/63.65	79.29/73.47	1.997/6.502	1.052/2.341	0.677/1.586	71.26/68.38	78.49/78.25
Std	0.012/0.024	0.009/0.007	0.007/0.014	0.000/0.000	0.001/0.000	0.013/0.035	0.015/0.013	0.009/0.011	0.000/0.000	0.000/0.000
Improv %	7.23%/9.72%	5.34%/3.07%	2.91%/5.72%	1.05%/0.73%	2.23%/0.70%	5.45%/2.15%	6.65%/9.37%	3.56%/4.74%	0.91%/2.97%	0.77%/0.88%
HGCN	1.337/2.285	0.951/1.138	0.971/1.200	76.04/62.26	75.68/69.64	2.765/7.849	1.159/1.794	0.661/1.277	67.57/62.31	74.67/73.53
HGCN w/P	1.282/2.124	0.879/1.036	0.921/1.104	76.70/63.25	77.41/72.76	2.609/7.781	1.092/1.682	0.637/1.146	69.17/65.7	75.87/75.32
Std	0.027/0.019	0.016/0.009	0.017/0.028	0.003/0.002	0.009/0.005	0.013/0.035	0.028/0.031	0.006/0.024	0.007/0.005	0.003/0.004
Improv %	4.11%/7.05%	7.57%/8.96%	5.15%/8.00%	0.87%/1.59%	2.29%/4.48%	5.64%/0.87%	5.78%/6.24%	3.63%/10.2%	2.37%/5.44%	1.61%/2.43%

Additionally, hyperbolic and spherical space embeddings demonstrate greater performance improvements compared to Euclidean methods (*i.e.*, Euclidean and complex space). Notably, the embedding derived from the product space yields the most substantial benefit for both urban flow forecasting and urban event prediction. Such result is consistent with their state-of-art performance in link prediction task. It indicates that explicitly representing urban structures is helpful for urban knowledge extraction and can be further explored to develop downstream tasks performances.

**Comparison of USTP Task Variants.** Table 6 shows the results of forecasting urban flow (*i.e.*, taxi service, bike trip and mobility prediction) for future period of 30 mins and predicting urban events (*i.e.*, urban crime and 311 service prediction) for future period of 120 mins. As can be seen, integrating product space UrbanKG embeddings consistently improves the accuracy of five tasks. The urban knowledge graph shows great potential (2%-10% improvement) in spatiotemporal flow prediction tasks, and it can also enhance (1%-5% improvement) urban event prediction. It is worth mentioning that the embeddings derived from UrbanKG are task-agnostic, where the downstream task is completely unknown. Such results indicate the UrbanKG embedding successfully captures general urban knowledge which is transferable among different USTP tasks.

**Comparison of USTP Model Variants.** It can be observed that integrating UrbanKG embeddings consistently improves the accuracy of six existing USTP models. The above results demonstrate well-extracted urban knowledge can still enhance existing USTP models (*e.g.*, ASTGCN and HGCN) from the feature representation scenario although they may already have sufficiently complex modules.

We provide implement details in Appendix A.4 and report more detailed results in Appendix A.5.

## 5 Related Work

**Domain Knowledge Graph Construction.** Knowledge graph has been widely studied in both academia and industry. In recent years, many open-source knowledge graphs have been released to

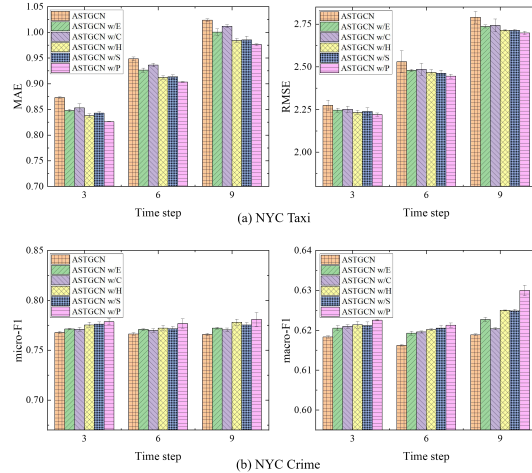


Figure 4: USTP performance comparison when incorporating embeddings derived by the best method of each space. (a) Performance on NYC Taxi. (b) Performance on NYC Crime.

improve applications in various domains. For example, CKGG [53], OpenBG [54], BioKG [55] and recent proposed ProteinKG25 [56] are used for education, business, biomedical and protein research field respectively. However, there is still no open-source knowledge graph for urban spatiotemporal prediction tasks in the urban computing field.

**Knowledge Graph Embedding.** Knowledge graph embedding aims to project entities and relations into low-dimensional vectors, which has been widely used for various KG-based applications. Overall, the knowledge graph embedding method can be categorized into two classes, the Euclidean embedding method and the non-Euclidean embedding method. The Euclidean embedding method derives KG embeddings in the Euclidean space. For example, TransE [30], TransH [57], TransR [58], RESCAL [59], DistMult [32], TuckER [35] and ConvE [60] utilize translation, matrix decomposition, or neural network to model entities and relations and derive embeddings. The non-Euclidean embedding method aims to capture more complicated structures in the latent space. For example, MuRP [16], AttH [17], ConE [18] and UltraE [61] model hierarchies in the hyperbolic or ultrahyperbolic space. Recently, several mixed curvature embedding methods [26, 37, 62] have been proposed to simultaneously encode diverse structures (*e.g.*, hierarchies and cycles) in a product space (*i.e.*, products of constant-curvature spaces). The above structure-aware non-Euclidean methods show great potential for modeling various high-order structures in UrbanKG.

**Knowledge-enhanced Urban Spatiotemporal Prediction.** Knowledge graph has been proven useful in various urban tasks, such as traffic flow prediction [63, 64, 65, 66], mobility prediction [7, 67, 68], site selection [69], city profiling [70, 71, 72, 73] and so on [74]. Their common approach involves manually constructing a UrbanKG, and then obtaining embeddings using classical methods like TransE [30] or TuckER [35]. Although some very recent methods [70, 71, 72] design task-relevant module to capture more granular urban knowledge, their UrbanKGs are still designed for specific tasks and are publicly not available, which discourages researchers from adopting it for their own work as building an UrbanKG from scratch is time-consuming and labor-intensive. In fact, several recent works [75, 8] are striving towards this problem. However, they only describe a UrbanKG construction scheme or system but do not offer an open-source UrbanKG.

## 6 Conclusion and Limitation

In this work, we proposed UUKG, a unified dataset for knowledge-enhanced urban spatiotemporal prediction. To the best of our knowledge, UUKG is the first open-source urban knowledge graph dataset compatible with various aligned USTP tasks in the urban computing field. Extensive experimental results demonstrate the universal advancement of UUKG in improving diverse USTP tasks. Additionally, we also prove the benefits of adopting state-of-art structure-aware UrbanKG embedding methods to further leverage rich high-order structures in UUKG.

Our work provides a unified UrbanKG construction framework but it has limitations in terms of the dataset generalizability, as all experiments were conducted in two US metropolises. In addition, we only consider concatenation operation for embedding fusion. It will be an interesting topic that how to suitably incorporate the learned embeddings to further enhance the performance of the urban spatiotemporal prediction. Despite the above limitations, we hope the constructed dataset can foster more extensive urban knowledge graph research and broad smart city application.

## 7 Maintenance Plan and Future Work

To ensure ease of access and future maintenance, the dataset and models evaluated in our paper are hosted on websites and cloud-based storage platforms. Specifically, we have created the UUKG homepage including detailed dataset descriptions and the evaluation code. The full dataset is available at Google Drive.

As an emerging building block, urban knowledge graph provides critical knowledge for urban spatiotemporal prediction models. Inevitably, more dataset, benchmarks and tools will be needed to facilitate its potential achievement. Therefore, we plan to continuously update UUKG by adding new urban entities derived from different data sources, new downstream tasks, and more friendly data usage toolkits and model interfaces. UUKG currently only contains the urban structural dataset for five types of USTP tasks. In the future, we will derive extra multi-modal data (*e.g.*, images, reviews) to enrich the UrbanKG and introduce more USTP tasks (*e.g.*, trajectory prediction and site selection).

## Acknowledgments and Disclosure of Funding

This research was supported in part by the National Natural Science Foundation of China under Grant No.62102110, the Alibaba Innovative Research Program (AIR). We appreciate the guidance provided by the team of Mr. Wang Qing, who is the Regional General Manager of Alibaba Cloud, in the Chongqing City Brain project.

## References

- [1] Fangzhou Sun, Abhishek Dubey, and Jules White. Dxnat—deep neural networks for explaining non-recurring traffic congestion. In *2017 IEEE International Conference on Big Data (IEEE BigData 2017), Boston, MA, USA, December 11-14, 2017*, pages 2141–2150, 2017.
- [2] Weiyu Cheng, Yanyan Shen, Yanmin Zhu, and Linpeng Huang. A neural attention model for urban air quality inference: Learning the weights of monitoring stations. In *Proceedings of the Thirty-Second AAAI Conference on Artificial Intelligence, AAAI 2018, USA, February 2-7, 2018*, pages 2151–2158, 2018.
- [3] Quanjun Chen, Xuan Song, Harutoshi Yamada, and Ryosuke Shibasaki. Learning deep representation from big and heterogeneous data for traffic accident inference. In *Proceedings of the Thirtieth AAAI Conference on Artificial Intelligence, February 12-17, 2016, Phoenix, Arizona, USA*, pages 338–344, 2016.
- [4] Xu Geng, Yilun Jin, Zhengfei Zheng, Yu Yang, Yexin Li, Han Tian, Peibo Duan, Leye Wang, Jiannong Cao, Hai Yang, et al. Citynet: A multi-city multi-modal dataset for smart city applications. *arXiv preprint arXiv:2106.15802*, 2021.
- [5] Lisa Tompson, Shane D. Johnson, Matthew P. J. Ashby, Chloe Perkins, and Phil Edwards. Uk open source crime data: accuracy and possibilities for research. *Cartography and Geographic Information Science*, pages 111–97, 2015.
- [6] Longbiao Chen, Daqing Zhang, Gang Pan, Xiaojuan Ma, Dingqi Yang, Kostadin Kushlev, Wangsheng Zhang, and Shijian Li. Bike sharing station placement leveraging heterogeneous urban open data. In *Proceedings of the 2015 ACM International Joint Conference on Pervasive and Ubiquitous Computing, UbiComp 2015, Osaka, Japan, September 7-11, 2015*, pages 571–575, 2015.
- [7] Huandong Wang, Qiaohong Yu, Yu Liu, Depeng Jin, and Yong Li. Spatio-temporal urban knowledge graph enabled mobility prediction. *Proc. ACM Interact. Mob. Wearable Ubiquitous Technol.*, pages 184:1–184:24, 2021.
- [8] Yu Liu, Jingtao Ding, and Yong Li. Developing knowledge graph based system for urban computing. In *Proceedings of the 1st ACM SIGSPATIAL International Workshop on Geospatial Knowledge Graphs*, pages 3–7, 2022.
- [9] Jintao Ke, Hai Yang, Hongyu Zheng, Xiqun Chen, Yitian Jia, Pinghua Gong, and Jieping Ye. Hexagon-based convolutional neural network for supply-demand forecasting of ride-sourcing services. *IEEE Trans. Intell. Transp. Syst.*, pages 4160–4173, 2019.
- [10] Junbo Zhang, Yu Zheng, Dekang Qi, Ruiyuan Li, and Xiuwen Yi. Dnn-based prediction model for spatio-temporal data. In *Proceedings of the 24th ACM SIGSPATIAL International Conference on Advances in Geographic Information Systems, GIS 2016, Burlingame, California, USA, October 31 - November 3, 2016*, pages 92:1–92:4, 2016.
- [11] Honglei Ren, You Song, Jingwen Wang, Yucheng Hu, and Jinzhi Lei. A deep learning approach to the citywide traffic accident risk prediction. In *21st International Conference on Intelligent Transportation Systems, ITSC 2018, Maui, HI, USA, November 4-7, 2018*, pages 3346–3351, 2017.
- [12] Xiaolei Ma, Haiyang Yu, Yunpeng Wang, and Yinhai Wang. Large-scale transportation network congestion evolution prediction using deep learning theory. *PLoS one*, page e0119044, 2015.
- [13] Mingqi Lv, Zhaoxiong Hong, Ling Chen, Tieming Chen, Tiantian Zhu, and Shouling Ji. Temporal multi-graph convolutional network for traffic flow prediction. *IEEE Transactions on Intelligent Transportation Systems*, pages 3337–3348, 2020.

- [14] Hongjian Wang, Daniel Kifer, Corina Graif, and Zhenhui Jessie Li. Crime rate inference with big data. In *Proceedings of the 22nd ACM SIGKDD International Conference on Knowledge Discovery and Data Mining, San Francisco, CA, USA, August 13-17, 2016*, pages 635–644, 2016.
- [15] Shuai Xu, Xiaoming Fu, Dechang Pi, and Zhuo Ma. Inferring individual human mobility from sparse check-in data: a temporal-context-aware approach. *IEEE Transactions on Computational Social Systems*, pages 1–12, 2022.
- [16] Ivana Balazevic, Carl Allen, and Timothy Hospedales. Multi-relational poincaré graph embeddings. In *Advances in Neural Information Processing Systems 32: Annual Conference on Neural Information Processing Systems 2019, NeurIPS 2019, December 8-14, 2019, Vancouver, BC, Canada*, pages 4465–4475, 2019.
- [17] Ines Chami, Adva Wolf, Da-Cheng Juan, Frederic Sala, Sujith Ravi, and Christopher Ré. Low-dimensional hyperbolic knowledge graph embeddings. In *Proceedings of the 58th Annual Meeting of the Association for Computational Linguistics, ACL 2020, Online, July 5-10, 2020*, pages 6901–6914, 2020.
- [18] Yushi Bai, Zhitao Ying, Hongyu Ren, and Jure Leskovec. Modeling heterogeneous hierarchies with relation-specific hyperbolic cones. In *Advances in Neural Information Processing Systems 34: Annual Conference on Neural Information Processing Systems 2021, NeurIPS 2021, December 6-14, 2021, virtual*, pages 12316–12327, 2021.
- [19] Ines Chami, Zhitao Ying, Christopher Ré, and Jure Leskovec. Hyperbolic graph convolutional neural networks. In *Advances in neural information processing systems*, 2019.
- [20] Cornelia Druțu and Michael Kapovich. *Geometric group theory*, volume 63. 2018.
- [21] Mikhael Gromov. *Hyperbolic groups*. 1987.
- [22] Frederic Sala, Christopher De Sa, Albert Gu, and Christopher Ré. Representation tradeoffs for hyperbolic embeddings. In *Proceedings of the 35th International Conference on Machine Learning, ICML 2018, Stockholmsmässan, Stockholm, Sweden, July 10-15, 2018*, pages 4457–4466, 2018.
- [23] Han Xiao, Minlie Huang, and Xiaoyan Zhu. From one point to a manifold: Knowledge graph embedding for precise link prediction. *arXiv preprint arXiv:1512.04792*, 2015.
- [24] Yu Meng, Jiaxin Huang, Guangyuan Wang, Chao Zhang, Honglei Zhuang, Lance Kaplan, and Jiawei Han. Spherical text embedding. In *Advances in neural information processing systems*, 2019.
- [25] Jake Topping, Francesco Di Giovanni, Benjamin Paul Chamberlain, Xiaowen Dong, and Michael M Bronstein. Understanding over-squashing and bottlenecks on graphs via curvature. *arXiv preprint arXiv:2111.14522*, 2021.
- [26] Shen Wang, Xiaokai Wei, Cicero Nogueira Nogueira dos Santos, Zhiguo Wang, Ramesh Nallapati, Andrew Arnold, Bing Xiang, Philip S Yu, and Isabel F Cruz. Mixed-curvature multi-relational graph neural network for knowledge graph completion. In *WWW '21: The Web Conference 2021, Virtual Event / Ljubljana, Slovenia, April 19-23, 2021*, pages 1761–1771, 2021.
- [27] Antoine Bordes, Jason Weston, Ronan Collobert, and Yoshua Bengio. Learning structured embeddings of knowledge bases. In *Proceedings of the Twenty-Fifth AAAI Conference on Artificial Intelligence, AAAI 2011, San Francisco, California, USA, August 7-11, 2011*, 2011.
- [28] Timothée Lacroix, Nicolas Usunier, and Guillaume Obozinski. Canonical tensor decomposition for knowledge base completion. In *Proceedings of the 35th International Conference on Machine Learning, ICML 2018, Stockholmsmässan, Stockholm, Sweden, July 10-15, 2018*, pages 2869–2878, 2018.
- [29] Rakesh Agrawal, Sreenivas Gollapudi, Alan Halverson, and Samuel Ieong. Diversifying search results. In *Proceedings of the Second International Conference on Web Search and Web Data Mining, WSDM 2009, Barcelona, Spain, February 9-11, 2009*, pages 5–14, 2009.
- [30] Antoine Bordes, Nicolas Usunier, Alberto Garcia-Duran, Jason Weston, and Oksana Yakhnenko. Translating embeddings for modeling multi-relational data. In *Advances in Neural Information Processing Systems 26: Annual Conference on Neural Information Processing Systems 2013, December 5-8, 2013, Lake Tahoe, Nevada, United States*, pages 2787–2795, 2013.

- [31] Zixuan Yuan, Hao Liu, Junming Liu, Yanchi Liu, Yang Yang, Renjun Hu, and Hui Xiong. Incremental spatio-temporal graph learning for online query-poi matching. In *Proceedings of the Web Conference 2021*, pages 1586–1597, 2021.
- [32] Bishan Yang, Wen-tau Yih, Xiaodong He, Jianfeng Gao, and Li Deng. Embedding entities and relations for learning and inference in knowledge bases. *arXiv preprint arXiv:1412.6575*, 2014.
- [33] Théo Trouillon, Johannes Welbl, Sebastian Riedel, Éric Gaussier, and Guillaume Bouchard. Complex embeddings for simple link prediction. In *Proceedings of the 33rd International Conference on Machine Learning, ICML 2016, New York City, NY, USA, June 19-24, 2016*, pages 2071–2080, 2016.
- [34] Zhiqing Sun, Zhi-Hong Deng, Jian-Yun Nie, and Jian Tang. Rotate: knowledge graph embedding by relational rotation in complex space. *arXiv preprint arXiv:1902.10197*, 2019.
- [35] Ivana Balažević, Carl Allen, and Timothy M Hospedales. Tucker: Tensor factorization for knowledge graph completion. In *Proceedings of the 2019 Conference on Empirical Methods in Natural Language Processing and the 9th International Joint Conference on Natural Language Processing, EMNLP-IJCNLP 2019, Hong Kong, China, November 3-7, 2019*, pages 5184–5193, 2019.
- [36] Zongsheng Cao, Qianqian Xu, Zhiyong Yang, Xiaochun Cao, and Qingming Huang. Dual quaternion knowledge graph embeddings. In *Proceedings of the AAAI conference on artificial intelligence*, volume 35, pages 6894–6902, 2021.
- [37] Zongsheng Cao, Qianqian Xu, Zhiyong Yang, Xiaochun Cao, and Qingming Huang. Geometry interaction knowledge graph embeddings. In *Thirty-Sixth AAAI Conference on Artificial Intelligence, AAAI 2022, Virtual, February 22 - March 1, 2022*, pages 5521–5529, 2022.
- [38] Noel Cressie and Christopher K Wikle. *Statistics for spatio-temporal data*. John Wiley & Sons, 2015.
- [39] Jie Feng, Yong Li, Chao Zhang, Funing Sun, Fanchao Meng, Ang Guo, and Depeng Jin. Deepmove: predicting human mobility with attentional recurrent networks. In *Proceedings of the 2018 World Wide Web Conference, WWW 2018, Lyon, France, April 23-27, 2018*, pages 1459–1468, 2018.
- [40] Chao Huang, Junbo Zhang, Yu Zheng, and Nitesh V Chawla. Deepcrime: Attentive hierarchical recurrent networks for crime prediction. In *Proceedings of the 27th ACM International Conference on Information and Knowledge Management, CIKM 2018, Torino, Italy, October 22-26, 2018*, pages 1423–1432, 2018.
- [41] Scott L Minkoff. Nyc 311: A tract-level analysis of citizen–government contacting in new york city. *Urban Affairs Review*, 52(2):211–246, 2016.
- [42] Cort J Willmott and Kenji Matsuura. Advantages of the mean absolute error (mae) over the root mean square error (rmse) in assessing average model performance. *Climate research*, pages 79–82, 2005.
- [43] Aditya Grover and Jure Leskovec. node2vec: Scalable feature learning for networks. In *Proceedings of the 22nd ACM SIGKDD international conference on Knowledge discovery and data mining*, pages 855–864, 2016.
- [44] Kyunghyun Cho, Bart Van Merriënboer, Dzmitry Bahdanau, and Yoshua Bengio. On the properties of neural machine translation: Encoder-decoder approaches. In *Proceedings of SSST@EMNLP 2014, Eighth Workshop on Syntax, Semantics and Structure in Statistical Translation, Doha, Qatar, 25 October 2014*, pages 103–111, 2014.
- [45] Geoffrey E Hinton, Alex Krizhevsky, and Sida D Wang. Transforming auto-encoders. In *Artificial Neural Networks and Machine Learning - ICANN 2011 - 21st International Conference on Artificial Neural Networks, Espoo, Finland, June 14-17, 2011, Proceedings, Part I*, pages 44–51, 2011.
- [46] Sepp Hochreiter and Jürgen Schmidhuber. Long short-term memory. *Neural computation*, 9(8):1735–1780, 1997.
- [47] Bing Yu, Haoteng Yin, and Zhanxing Zhu. Spatio-temporal graph convolutional networks: A deep learning framework for traffic forecasting. In *Proceedings of the Twenty-Seventh International Joint Conference on Artificial Intelligence, IJCAI 2018, July 13-19, 2018, Stockholm, Sweden*, pages 3634–3640, 2017.

- [48] Shengnan Guo, Youfang Lin, Ning Feng, Chao Song, and Huaiyu Wan. Attention based spatial-temporal graph convolutional networks for traffic flow forecasting. In *The Thirty-Third AAAI Conference on Artificial Intelligence, AAAI 2019, Honolulu, Hawaii, USA, January 27 - February 1, 2019*, pages 922–929, 2019.
- [49] Ling Zhao, Yujiao Song, Chao Zhang, Yu Liu, Pu Wang, Tao Lin, Min Deng, and Haifeng Li. T-gcn: A temporal graph convolutional network for traffic prediction. *IEEE Trans. Intell. Transp. Syst.*, pages 3848–3858, 2019.
- [50] Zonghan Wu, Shirui Pan, Guodong Long, Jing Jiang, Xiaojun Chang, and Chengqi Zhang. Connecting the dots: Multivariate time series forecasting with graph neural networks. In *Proceedings of the 26th ACM SIGKDD international conference on knowledge discovery & data mining*, pages 753–763, 2020.
- [51] Lei Bai, Lina Yao, Can Li, Xianzhi Wang, and Can Wang. Adaptive graph convolutional recurrent network for traffic forecasting. In *Advances in neural information processing systems*, volume 33, pages 17804–17815, 2020.
- [52] Kan Guo, Yongli Hu, Yanfeng Sun, Sean Qian, Junbin Gao, and Baocai Yin. Hierarchical graph convolution network for traffic forecasting. In *Proceedings of the AAAI conference on artificial intelligence*, volume 35, pages 151–159, 2021.
- [53] Yulin Shen, Ziheng Chen, Gong Cheng, and Yuzhong Qu. Ckkg: A chinese knowledge graph for high-school geography education and beyond. In *The Semantic Web - ISWC 2021 - 20th International Semantic Web Conference, ISWC 2021, Virtual Event, October 24-28, 2021, Proceedings*, pages 429–445, 2021.
- [54] Shumin Deng, Hui Chen, Zhoubo Li, Feiyu Xiong, Qiang Chen, Mosha Chen, Xiangwen Liu, Jiaoyan Chen, Jeff Z Pan, Huajun Chen, et al. Construction and applications of open business knowledge graph. *arXiv preprint arXiv:2209.15214*, 2022.
- [55] Brian Walsh, Sameh K Mohamed, and Vít Nováček. Biokg: A knowledge graph for relational learning on biological data. In *CIKM '20: The 29th ACM International Conference on Information and Knowledge Management, Virtual Event, Ireland, October 19-23, 2020*, pages 3173–3180, 2020.
- [56] Ningyu Zhang, Zhen Bi, Xiaozhuan Liang, Siyuan Cheng, Haosen Hong, Shumin Deng, Jiazhang Lian, Qiang Zhang, and Huajun Chen. Ontoprotein: Protein pretraining with gene ontology embedding. *arXiv preprint arXiv:2201.11147*, 2022.
- [57] Zhen Wang, Jianwen Zhang, Jianlin Feng, and Zheng Chen. Knowledge graph embedding by translating on hyperplanes. In *Proceedings of the Twenty-Eighth AAAI Conference on Artificial Intelligence, July 27 -31, 2014, Québec City, Québec, Canada*, pages 1112–1119, 2014.
- [58] Yankai Lin, Zhiyuan Liu, Maosong Sun, Yang Liu, and Xuan Zhu. Learning entity and relation embeddings for knowledge graph completion. In *Proceedings of the Twenty-Ninth AAAI Conference on Artificial Intelligence, January 25-30, 2015, Austin, Texas, USA*, pages 2181–2187, 2015.
- [59] Maximilian Nickel, Volker Tresp, and Hans-Peter Kriegel. A three-way model for collective learning on multi-relational data. In *Proceedings of the 28th International Conference on Machine Learning, ICML 2011, Bellevue, Washington, USA, June 28 - July 2, 2011*, pages 809–816, 2011.
- [60] Tim Dettmers, Pasquale Minervini, Pontus Stenetorp, and Sebastian Riedel. Convolutional 2d knowledge graph embeddings. In *Proceedings of the Thirty-Second AAAI Conference on Artificial Intelligence, AAAI 2018, New Orleans, Louisiana, USA, February 2-7, 2018*, pages 1811–1818, 2018.
- [61] Bo Xiong, Shichao Zhu, Mojtaba Nayyeri, Chengjin Xu, Shirui Pan, Chuan Zhou, and Steffen Staab. Ultrahyperbolic knowledge graph embeddings. In *KDD '22: The 28th ACM SIGKDD Conference on Knowledge Discovery and Data Mining, Washington, DC, USA, August 14 - 18, 2022*, pages 2130–2139, 2022.
- [62] Roshni G. Iyer, Yunsheng Bai, Wei Wang, and Yizhou Sun. Dual-geometric space embedding model for two-view knowledge graphs. In *KDD '22: The 28th ACM SIGKDD Conference on Knowledge Discovery and Data Mining, Washington, DC, USA, August 14 - 18, 2022*, pages 676–686, 2022.

- [63] Chengbiao Yang and Guilin Qi. An urban traffic knowledge graph-driven spatial-temporal graph convolutional network for traffic flow prediction. In *Proceedings of the 11th International Joint Conference on Knowledge Graphs*, pages 110–114, 2022.
- [64] Jiyuan Tan, Qianqian Qiu, Weiwei Guo, and Tingshuai Li. Research on the construction of a knowledge graph and knowledge reasoning model in the field of urban traffic. *Sustainability*, 13(6):3191, 2021.
- [65] Jia Liu, Tianrui Li, Shenggong Ji, Peng Xie, Shengdong Du, Fei Teng, and Junbo Zhang. Urban flow pattern mining based on multi-source heterogeneous data fusion and knowledge graph embedding. *IEEE Transactions on Knowledge and Data Engineering*, 2021.
- [66] Ling Zhao, Hanhan Deng, Linyao Qiu, Sumin Li, Zhixiang Hou, Hai Sun, and Yun Chen. Urban multi-source spatio-temporal data analysis aware knowledge graph embedding. *Symmetry*, 12(2):199, 2020.
- [67] Chenyi Zhuang, Nicholas Jing Yuan, Ruihua Song, Xing Xie, and Qiang Ma. Understanding people lifestyles: Construction of urban movement knowledge graph from gps trajectory. In *Proceedings of the Twenty-Sixth International Joint Conference on Artificial Intelligence, IJCAI 2017, Melbourne, Australia, August 19-25, 2017*, pages 3616–3623, 2017.
- [68] Haoran Xin, Xinjiang Lu, Tong Xu, Hao Liu, Jingjing Gu, Dejing Dou, and Hui Xiong. Out-of-town recommendation with travel intention modeling. In *Proceedings of the AAAI Conference on Artificial Intelligence*, volume 35, pages 4529–4536, 2021.
- [69] Yu Liu, Jingtao Ding, and Yong Li. Knowledge-driven site selection via urban knowledge graph. *arXiv preprint arXiv:2111.00787*, 2021.
- [70] Zhilun Zhou, Yu Liu, Jingtao Ding, Depeng Jin, and Yong Li. Hierarchical knowledge graph learning enabled socioeconomic indicator prediction in location-based social network. In *Proceedings of the ACM Web Conference*, pages 122–132, 2023.
- [71] Yu Liu, Zhilun Zhou, Yong Li, and Depeng Jin. Urban knowledge graph aided mobile user profiling. *ACM Trans. Knowl. Discov. Data*, 1(1), 2023.
- [72] Yu Liu, Xin Zhang, Jingtao Ding, Yanxin Xi, and Yong Li. Knowledge-infused contrastive learning for urban imagery-based socioeconomic prediction. In *Proceedings of the ACM Web Conference*, pages 4150–4160, 2023.
- [73] Weijia Zhang, Hao Liu, Lijun Zha, Hengshu Zhu, Ji Liu, Dejing Dou, and Hui Xiong. Mugrep: A multi-task hierarchical graph representation learning framework for real estate appraisal. In *Proceedings of the 27th ACM SIGKDD Conference on Knowledge Discovery & Data Mining*, pages 3937–3947, 2021.
- [74] Qingyan Zhu, Yize Chen, Hao Wang, Zhenyu Zeng, and Hao Liu. A knowledge-enhanced framework for imitative transportation trajectory generation. In *2022 IEEE International Conference on Data Mining (ICDM)*, pages 823–832. IEEE, 2022.
- [75] Yu Liu, Jingtao Ding, Yanjie Fu, and Yong Li. Urbankg: An urban knowledge graph system. *ACM Transactions on Intelligent Systems and Technology*, 14(4):1–25, 2023.
- [76] Diederik P Kingma and Jimmy Ba. Adam: A method for stochastic optimization. *arXiv preprint arXiv:1412.6980*, 2014.

## A Appendix

### A.1 Datasheet for UrbanKG Dataset

We have presented the UrbanKG dataset construction progress in Section 2. The detailed statistics of entities of UrbanKG are shown in Table 7. As can be seen, we define 15 categories of POI including finance, parking area, shopping, catering, and so on. In addition, we preserve six-types of most frequent road segments including motorway (expressway or river crossing tunnels), primary traffic road, secondary traffic road, tertiary traffic road, residential traffic road, and trunk (branch roads such as expressway outbound bypass roads). We also keep five-types of frequent road junction including motorway junction (road junction in expressway or river-crossing tunnel), traffic signal (road junction having traffic light), turning circle (road junction which is a roundabout), stop (road junction having stop signal) and crossing (road junction with no special type).

### A.2 UrbanKG Embedding Implement Details and Detailed Results

We implement all models by using PyTorch. All experiments are conducted on eight NVIDIA RTX 3090 GPUs. We use Adam [76] as the optimizer and the negative sampling size is fixed to 50. We conduct a grid search to select learning rate in  $\{0.001, 0.005, 0.01, 0.05, 0.1\}$  and batch size in  $\{512, 1024, 2048, 4096, 5120\}$ . The best hyper-parameters are selected by early stop on the validation sets and we report them in Table 8. The performance of different models in high dimensional setting ( $d = 150$ ) is similar with our analysis in Section 3.3 and we report the detailed results in Table 9.

### A.3 Datasheet for USTP Dataset

#### A.3.1 Dataset Construction

In this section, we detail the datasets construction process of five USTP tasks step by step.

**Taxi Service:** (1) Data collection: NYC TCL<sup>6</sup> provides yellow taxi trip records which could cover 260 areas in NYC, thus we choose it to construct our dataset. A taxi trip record contains pick-up time, pick-up location, drop-off time and drop-off locations. For example,  $[2020/4/1/00:15, (40.72, -73.98), 2020/4/1/09:10, (40.73, -73.97)]$  is a taxi trip record. (2) Dataset construction: the inflow and outflow of an area can be calculated by counting the amount of taxis entering and leaving within a period of time. For NYC taxi service prediction, we count the inflow and outflow in each area every 30 minutes from 1st April to 31st June, 2020. For CHI taxi service prediction, we count the inflow and outflow in each area every 30 minutes from 1st April to 31st June, 2019. By the above steps, we obtain the spatio-temporal dataset of taxi service.

**Bike Trip:** (1) Data collection: Amazon S3<sup>7</sup> provides NYC bike trip data, which records the start and end points of the bike trip and has precise latitude and longitude. Every record contains the start time and end time. For example,  $[2020/4/1/4:20, (40.68, -74.01), 2020/4/1/4:26, (40.68, -73.99)]$  is a bike trip record. (2) Dataset construction: the inflow and outflow of a road can be calculated by counting the amount of bikes entering and leaving within a period of time. Due to the lack of bike flow data for most roads at each time step, we filter and sample roads to prevent excessive long tail issues. Specifically, for NYC bike trip prediction, we calculate the inflow and outflow on each road at 30-minute intervals from April 1st to June 31st, 2020. Subsequently, we select 2,500 roads from those with the highest bike flow values. For CHI bike trip prediction, we count the inflow and outflow in each road every 30 minutes from 1st April to 31st June, 2019. Next, we select 1,500 roads from those with the highest bike flow values. Through these steps, we obtain the spatio-temporal datasets for bike trip prediction.

**Human Mobility:** We construct human mobility dataset based on taxi service and bike trip data. The inflow and outflow of a POI can be calculated by counting the number of taxi passengers, taxi drivers and bikers, who enter and leave within a period of time.

<sup>6</sup><https://www.nyc.gov/site/tlc/about/tlc-trip-record-data.page>

<sup>7</sup><https://s3.amazonaws.com/tripdata/index.html>

Table 7: Information for category of POI, Road and Junction in UrbanKG.

Entity	Description	Quantity	
		NYC	CHI
PC	catering	501	280
	corporation	821	1,042
	culture and education	2,296	2,352
	domestic service	155	15
	finance	112	64
	governments and organization	538	143
	medical and health	337	237
	parking area	31,484	10,545
	place of workshop	1,592	1,057
	public service	1,609	1,141
	residential area	21,166	9,885
	scenic spot	164	802
	shopping	1,362	2,690
RC	sports and leisure	143	885
	transportation	185	450
	motorway	2,523	1,011
	primary	7,173	4,289
	secondary	12,717	13,024
	tertiary	10,964	7,385
JC	residential	77,024	45,775
	trunk	524	100
	crossing	45,182	32,158
	motorway junction	704	250
	stop	1,437	155
	traffic signal	14,677	3,902
	turning circle	441	626

Due to the absence of mobility flow data for most POIs at each time step, we filter and sample POIs to avoid excessive long tail issues. For NYC mobility prediction, we calculate the inflow and outflow at each POI at 30-minute intervals from April 1st to June 31st, 2020. Then, we choose 1,600 roads from those with the highest mobility flow values. For CHI mobility prediction, we measure the inflow and outflow at each POI at 30-minute intervals from April 1st to June 31st, 2019. Subsequently, we select 1,000 POIs from those with the highest mobility flow values. By the above steps, we obtain the spatio-temporal dataset of POI-level mobility prediction.

**Crime:** (1) Data collection: NYC OpenData<sup>8</sup> provides crime occurrence data, which includes all valid felony, misdemeanor and violation crimes reported to the New York City Police Department (NYPD). Every crime record contains crime type, time, latitude and longitude. For example,  $[FELONY, 2021/12/17/22:13, (40.64, -73.90)]$  is a crime record. (2) Dataset construction: the crime label for an area can be established by examining if any criminal activities occur within a designated time frame. Due to the sparsity of crime occurrence, we create the crime label in each area every 120 minutes from 1st Jan to 31st Dec, 2021. By the above steps,

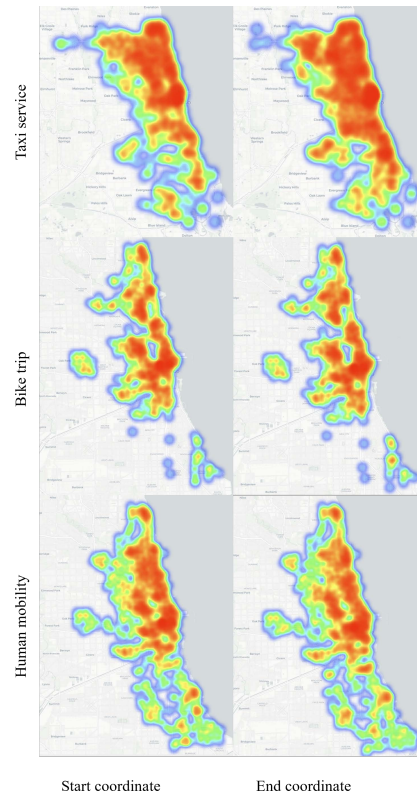


Figure 5: Heat map of the start and end coordinate of taxi, bike, and human trip in CHI USTP dataset.

<sup>8</sup><https://data.cityofnewyork.us/Public-Safety/NYPD-Complaint-Data-Historic/qgea-i56i>

Table 8: Best hyperparameters of different UrbanKG embedding methods.

Space	Model	Learning rate	Optimizer	Batch size	Negative samples
Euclidean models	TransE	0.001	Adam	2048	50
	DisMult	0.0005	Adam	2048	50
	MuRE	0.001	Adam	4096	50
	TuckER	0.0005	Adam	1024	50
	RotatE	0.05	Adagrad	2048	50
	CompIEEx	0.05	Adagrad	2048	50
	QuatE	0.001	Adam	2048	50
Non-Euclidean models	MuRS	0.001	Adam	4096	50
	MuRP	0.001	Adam	4096	50
	RotH	0.001	Adam	4096	50
	RefH	0.05	Adagrad	4096	50
	AttH	0.001	Adam	4096	50
	ConE	0.001	Adam	4096	50
	M2GNN	0.001	Adam	4096	50
	GIE	0.001	Adam	4096	50

Table 9: Overall link prediction results for high-dimensional embeddings  $d = 150$ .

Type	Space	Model	NYC				CHI			
			MRR	Hits@10	Hits@3	Hits@1	MRR	Hits@10	Hits@3	Hits@1
Euclidean models	E	TransE	.547	.592	.553	.501	.517	.582	.544	.475
	E	DisMult	.462	.514	.477	.402	.432	.499	.485	.426
	E	MuRE	.556	.632	.581	.513	.524	.642	.565	.462
	E	TuckER	.532	.627	.584	.492	.513	.602	.547	.466
	C	RotatE	.302	.395	.342	.265	.344	.412	.367	.291
	C	CompIEEx	.289	.388	.337	.253	.352	.417	.365	.297
	C	QuatE	.355	.421	.386	.322	.431	.514	.458	.396
Non-Euclidean models	S	MuRS	.566	.647	.585	.506	.538	.649	.570	.471
	H	MuRP	.559	.639	.591	.512	.533	.643	.569	.477
	H	RotH	.571	.654	.594	.511	.546	.648	.573	.481
	H	RefH	.562	.636	.581	.509	.539	.642	.572	.477
	H	ATTH	.573	.656	.592	.513	.545	.647	.571	.489
	H	ConE	.565	.637	.588	.511	.538	.639	.566	.485
	P	M2GNN	.578	.642	.601	.523	.552	.647	.582	.503
	P	GIE	.587	.651	.607	.532	.561	.656	.596	.513

we obtain the spatio-temporal dataset of crime prediction.

**311 Service:** (1) Data collection: NYC 311 <sup>9</sup> provides and updates daily 311 service request automatically, which includes air quality issue, illegal parking and so on. Every 311 service record contains complaint type, created date, latitude and longitude. For example, *[Illegal parking, 2021/06/27/12:42, (40.88, -73.89)]* is a 311 service record. (2) Dataset construction: the 311 service label for an area can be obtained by examining if any 311 service activities occur within a designated time frame. We create the 311 service label in each area every 120 minutes from 1st Jan to 31st Dec, 2021. By the above steps, we obtain the spatio-temporal dataset of 311 service prediction.

### A.3.2 Dataset Visualization

In addition, we take Chicago as an example to visualize the spatial and temporal distribution of various USTP dataset and the pattern in New York is similar. As shown in Figure 5, we can see the start points and end points of the three urban trip (*i.e.*, taxi service, bike trip, human mobility, crime and 311 service). Figure 6 also shows the spatial distribution of crime events and 311 service complaints. We illustrates the temporal distribution of the these five tasks in Figure 7.

<sup>9</sup><https://portal.311.nyc.gov/>

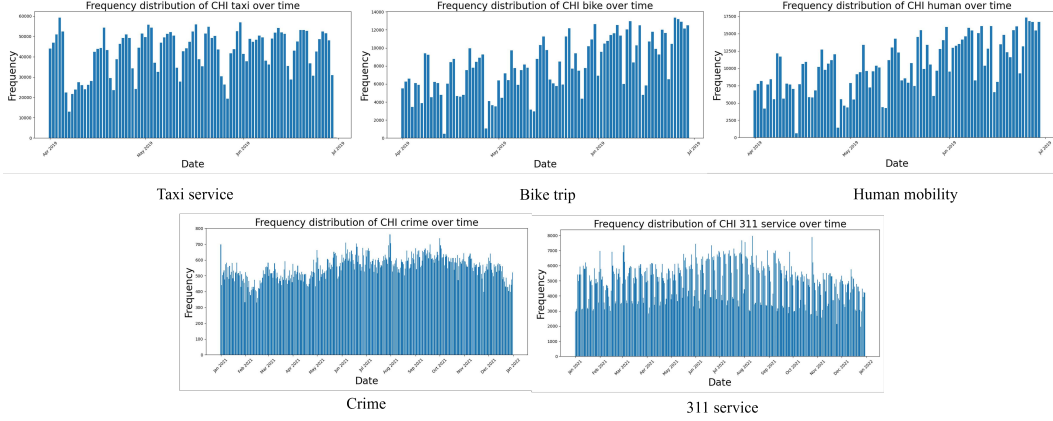


Figure 7: Frequency histogram of taxi, bike, human trip, crime and 311 service event in CHI USTP dataset.

#### A.4 USTP Models Implement Details

We split data with a ratio of 7:1:2 into training sets, validation sets and test sets. We use historical 12 time steps to predict the future 1 to 12 time steps. We implement all the models and methods in pytorch with eight NVIDIA RTX 3090 GPUs. We use Adam [76] as the optimizer and the batch size is fixed to 64. The best model hyperparameters are determined using early stopping on the validation sets. The final configurations for each model are saved as JSON files in our open-source code <https://github.com/usail-hkust/UUKG/>.

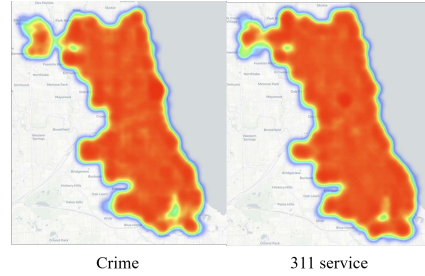


Figure 6: Heat map of the event coordinate of crime and 311 service.

#### A.5 USTP Detailed Results

Section 4 has demonstrates effectiveness of product space UrbanKG embedding in improving diverse USTP tasks, this section provides more detailed results. Specifically, we compare the impact on downstream USTP task performance when product space embeddings of different dimensions (*i.e.*, 8, 16, 32, 64 and 128 dimensions) are used for downstream tasks.

**Comparison of UrbanKG Embedding dimensions.** We report the results of forecasting NYC taxi flow and NYC crime events for future 3, 6 and 9 time step. As shown in Figure 8, we present a comparison of performance gaps for USTP tasks using product embeddings of different dimensions. It is evident that the UrbanKG embedding improves USTP performance across a range of embedding dimensions from 8 to 128. Moreover, the performance improvement becomes less significant when the embedding dimension exceeds 32.

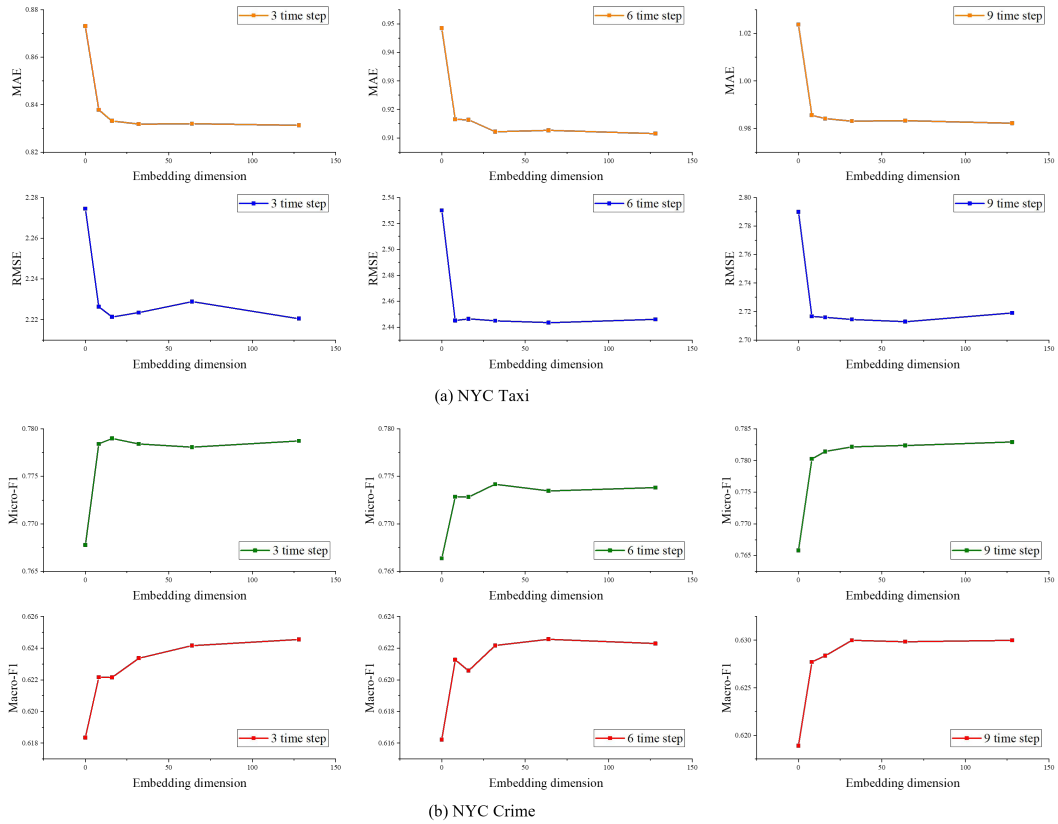


Figure 8: USTP performance comparison when incorporating product space embeddings with different dimension into ASTGCN model. The performance of embedding dimension '0' is the result is the ASTGCN model without UrbanKG embedding. (a) USTP Performance on NYC Taxi. (b) USTP Performance on NYC Crime.